15th International Plansee Seminar, Eds. G. Kneringer, P. Rödhammer and H. Wildner, Plansee Holding AG, Reutte (2001), Vol. 2

Fundamentals of Liquid Phase Sintering for Modern Cermets and Functionally Graded Cemented Carbonitrides (FGCC)

Limin Chen[1]*, Walter Lengauer[2], Peter Ettmayer[2],
Klaus Dreyer[3], Hans W. Daub[3] and Dieter Kassel[3]

[1] Austrian Research Center, Division of Materials Technology, A-2444, Austria

* Current address: SinterMet, LLC. West Hills Industrial Park, Kittanning, PA 16201, USA.

[2] Institute for Chemical Technology of Inorganic Materials
Vienna University of Technology, Getreidemarkt 9/161, A-1060, Austria

[3] WIDIA GmbH, Munchener Str. 90, D-45145 Essen, Germany

ABSTRACT

Metallurgical reactions and microstructure developments during sintering of modern cermets and functionally graded cemented carbonitrides (FGCC) were investigated by modern thermal and analytical methods such as mass spectrometer (MS), differential thermal analysis (DTA), differential scanning calorimeter (DSC), dilatometer (DIL), microscopy and analytical electronic microscopy with energy dispersive spectrometer (EDS). The complex phase reactions and phase equilibria in the multi-component system Ti/Mo/W/Ta/Nb/C,N-Co/Ni were studied. The melting behaviors in the systems of TiC-WC/MoC-Ni/Co, TiC-TiN-WC-Co and TiCN-TaC-WC-Co have been established. By better understanding of the mechanisms that govern the sintering processing and metallurgical reactions, new cermets and different types of functionally graded cemented carbonitrides (FGCC) with desired microstructures and properties were developed and fabricated.

Keywords: Functionally graded cemented carbonitrides, Cermets, Cutting tools, Phase diagram, Thermal analysis.

1. INTRODUCTION

The importance of introducing nitrogen in the form of TiN into TiC-Ni/Mo cermets was discovered by Kieffer et. al. around 1970 [1]. Systematic researches afterwards led to a new generation of modern cutting cermets, which is characterized by multi-components with TiC and TiN, or alternatively, TiCN as the basic ingredients. Additions of Mo_2C, WC, TaC, NbC and VC add up to 20-40 mass% of the total. The binder alloys usually contain Ni and Co on the order of 10-15 mass% but in varying relative amounts. The performance of the modern cutting cermets can match or even better than that of coated cemented carbides. Some excellent reviews on the modern cermets are given in the literature [2-5].

15th International Plansee Seminar, Eds. G. Kneringer, P. Rödhammer and H. Wildner, Plansee Holding AG, Reutte (2001), Vol. 2

As for the coated cemented carbides, the surface zone of the "state-of-the-art" substrate often features a Co-enriched and cubic-phase free layer (CFL). During interrupted machining, such CFL layer underneath the ceramic coatings absorbs most of the energy so that the impact resistance of the coated carbide grades is greatly improved. The CFL surface layer is usually prepared by a post-sintering treatment of nitrogen-containing alloys under (high) vacuum at cooling speeds less than 10 K/min. [6-10]. The denitrdation (i.e. decomposition of nitrides or carbonitrides) caused by vacuum treatment is believed to form the CFL character on the surface of the substrates.

The surface zone can also be modified into a unique structure with a gradation enriched in TiCN cubic phase and depleted in WC and Co/Ni binder. So called FGM (functionally graded material) cemented carbonitrides are sintered in a nitrogen-containing atmosphere. Inserts with as-sintered single or multi- FGM layers have been developed and were reported to perform better than the coated carbides [11-16]. In addition to the improvement of the cutting performance, very costly coating process may be eliminated by the new developed FGM technology. Saving potential is promising since coating process accounts for more than 15% of the total manufacturing costs while sintering process accounts for only 5% [17].

Nitrogen plays more and more critical role to develop new generation of cutting toll materials. However, with the addition of nitrogen (through carbonitrides, nitrides or nitrogen gas), the metallurgical reactions during sintering become much more complex and the sintering atmosphere has to be more accurately controlled [12-16, 18-19]. The cutting tool industry is still lacking in understanding the mechanisms of liquid phase sintering of nitrogen-containing cemented carbides. The present work approaches to carry out a systematic research in order to fill in these gaps.

EXPERIMENTAL PROCEDURES

Differential Thermal Analysis (DTA)

DTA was used to measure melting points of experimental alloys with 33 wt % binder metal content or higher. Highly pure re-crystallized alumina was used as a crucible material and a platinum alloy as a reference standard. The temperature was measured with a Pt/Rh thermocouple and the accuracy of the temperature measurement is estimated to be within ± 3°C by calibration against known melting points of high purity Cu and Cu-Ni alloys.

Differential Scanning Calorimeter (DSC) Measurements

Melting points of industrial alloys were measured by a DSC system (Netzsch DSC 404). This system monitors the ΔT signal representing the difference in temperature between a sample and an inert reference material as a function of temperature. The temperature was calibrated against the melting point of Au and the measurement error was within 1°C.

Dilatometer (DIL) Measurements

The shrinkage behaviors of the industrial alloys were monitored by a dilatometer (Netzsch DIL 402C, max. temperature 1600°C). The samples were heated under vacuum of $4\sim6\times10^{-4}$ mbar till 1300°C. The vacuum pump was then turned off. The gas pressure rose to a few mbar during sintering.

15th International Plansee Seminar, Eds. G. Kneringer, P. Rödhammer and H. Wildner, Plansee Holding AG, Reutte (2001), Vol. 2

Gas Analysis by A Mass Spectrometer (MS)

Gases CO and N_2 released during sintering were monitored by a system illustrated in Fig.1. In the MF furnace a high-pressure interface was inserted between the recipient and the quadrupole mass spectrometer system in order to be able to characterize the sintering atmosphere at pressures in the mbar ranges. This is necessary because a He gas stream has to be used to elute the gases from the crucible into the MS system. A gas flow system together with a second pump was used in order to sustain a constant pressure of 20 mbar. The ion fluxes of CO^+, N_2^+ and N^+ were recorded, calibrated against standard gas mixtures and introduced in a system of linear equations (because of the coincidence of N_2^+ and CO^+ at mass 28) for the CO and N_2 concentrations.

Solid-Liquid Reactions

"Solid compact - liquid metal" reaction couples were carried out by embedding a piece of hot-pressed carbide plate and Co or Ni powders in an alumina crucible. The reaction couples were heated up to 1550°C within 40 minutes in a BALZERS VSG 02 furnace equipped with a tungsten heating element under Ar atmosphere of 300 mbar. The electrical power of the device was turned off as soon as the samples had reached the vertex temperature of 1550°C. The specimens were then furnace cooled.

Microstructure Evaluation

Microstructures were investigated by optical microscope, scanning electron microscope (SEM, model JEOL JSM 6400) and scanning transmission electron microscope (STEM, model H-800). Quantitative compositional analysis was performed by energy dispersive spectroscopy (EDS) detectors attached to SEM and STEM.

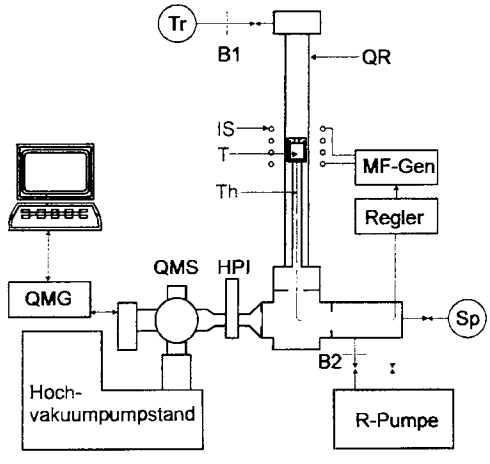

QMS	quadrupole mass spectrometer
QMG	QMS electronics
HPI	high pressure interface
Regler	temperature controller
MF-Gen	MF generator
IS	induction coil
T	crucible with sample
B1	orifice 1
B2	orifice 2
Tr	elution gas (He)
Sp	flushing gas
R-Pumpe	rotation pump
QR	silica tube
Th	thermo-element

Fig.1- Schematic illustration of MS gas analysis system

15th International Plansee Seminar, Eds. G. Kneringer, P. Rödhammer and H. Wildner, Plansee Holding AG, Reutte (2001), Vol. 2

RESULTS AND DISCUSSION

Melting Point Temperatures Measured by DTA

The onset points of DTA heating curves were used as melting point temperatures. The melting points of binary eutectic reactions: melts ⇒ Co (or Ni) + (Ti, W)C (or (Ti, Mo)C) were measured by DTA using experimental alloys with 90 mol % binder metals. The results are given in Fig.2 (a), (b), (c) and (d). Because of the high binder content, all alloy components dissolved in the liquid melt at maximum measurement temperature of about 1500°C. The addition of "MoC" does not change the melting points of TiC-Ni alloys, but decreases the melting points of TiC-Co alloys (see Fig.2 (a) and (c)). If WC is added, the melting points of TiC-Ni alloys will continuously increase from 1295°C to 1370°C (see Fig.2 (b)). The melting points of TiC-Co alloys increase to a maximum value and then decrease if TiC is replaced by WC (see Fig.2 (d)).

Almost one hundred samples of nitrogen-containing alloys with 33 wt% Co were measured by DTA. The results are summarized in Fig.2 (e) and (f). Some of the alloys were also observed by the microscope and/or SEM in order to study the phase existence. For alloys in the WC phase existing region, i.e. in the region of WC + (Ti,W)(C,N) + Co, the same melting point temperature of 1350°C was observed as shown in Fig.2 (e). For alloys in the (Ti,W)(C,N) + Co region without WC, the melting point temperatures of the alloys vary from 1350°C for high TiC containing alloys to 1450°C for high TiN containing alloys. The addition of TaC to the WC-TiCN-Co alloys did not change the melting point temperatures, but decreased the solution of WC in the (Ti,W,Ta)(C,N) cubic phase (see Fig.2 (f)).

Melting Behaviors of Some Industrial Alloys Measured By DSC

Industrial alloys contain much less amount of binder phase than the DTA experimental alloys. DSC was employed in order to measure the melting points of the industrial alloys accurately. The results are given in Table 1 and Fig.3.

Table 1- Onset and peak point temperatures of some industrial alloys measured by DSC

Alloys	Heating Phase; °C		Cooling Phase; °C		Phase Observed	Remarks
	Onset	Peak	Onset	Peak		
# 45	1347	1365	1355	1347	WC, Co	cemented carbide
# 62	1338/ 1382	1395	1391	1385	WC, Co/Ni	cemented carbide
# 32	1356	1367	1355	1347	WC, (Ti,W)C, Co	cemented carbide
# 35	1356	1367	1355	1344	WC, (Ti,W)(C,N), Co	cemented carbonitride
# 37	1358	1367	1351	1343	WC, TiN, Co	cemented carbonitride
# 44	1389	1404	1396	1383	WC, (Ti,W)(C,N), Co/Ni	TiCN cermet
# 42	1416	1426	1414	1404	(Ti,W)(C,N), Co/Ni	TiCN cermet
# 43	1410	1423	1370	1355	(Ti,W)(N,C), Co/Ni	TiN cermet

15th International Plansee Seminar, Eds. G. Kneringer, P. Rödhammer and H. Wildner, Plansee Holding AG, Reutte (2001), Vol. 2

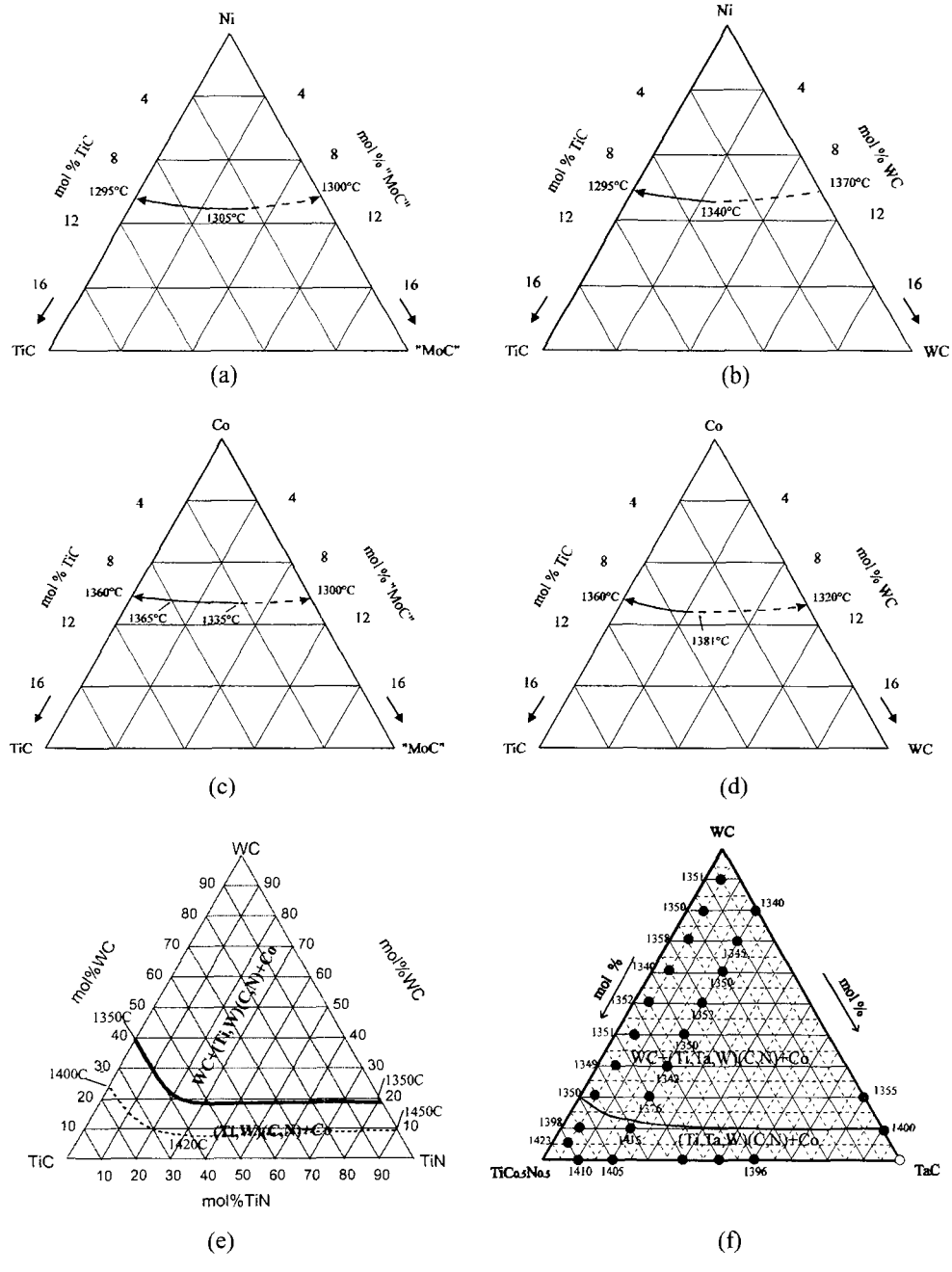

Fig.2- Melting point temperatures measured by DTA.

15th International Plansee Seminar, Eds. G. Kneringer, P. Rödhammer and H. Wildner, Plansee Holding AG, Reutte (2001), Vol. 2

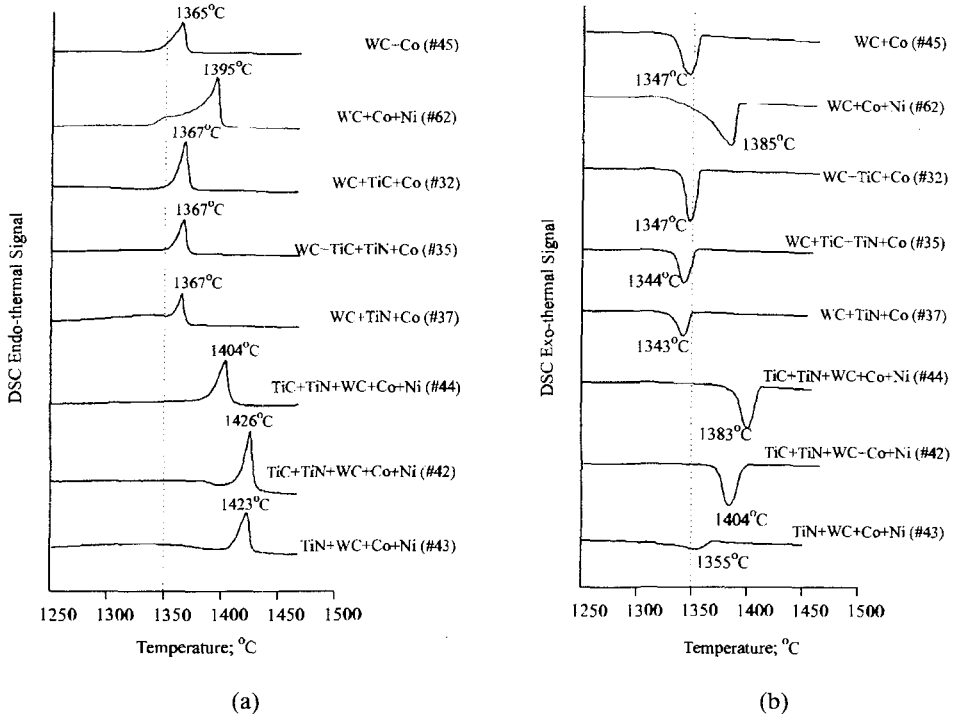

Fig.3- DSC curves of some industrial alloys, (a) heating phase and (b) cooling phase

DSC results coincide with DTA results very well. The compositions of alloys # 45, # 32, # 35 and # 37 are located in the three phase region of WC+(Ti,W)(C,N)+Co (see Fig.2 (e) and (f)). Regardless of their C/N ratios and Ti/W ratios, these alloys have almost the same onset point temperature of about 1350°C, which is also the same as the onset point temperatures of DTA experimental alloys (see Fig.2 (e)). Compared alloy # 62 with alloy # 45, alloy # 62 has two onset point temperatures and its melting range (1338-1395°C) is much broader than that of alloy # 45 (1347-1365°C). WC-Co alloy has a lower quasi-binary eutectic temperature (1320°C, see Fig.2 (b)) than WC-Ni alloy (1370°C, see Fig.2 (d)). During heating of the alloy # 62, WC react with Co at low temperature to form liquid phase which is reflected by the first onset point on the DSC curve. The second onset point temperature of 1382°C reflects the second reaction: WC + Ni $\Rightarrow$ melt at high temperature. Since cermet alloy # 44 also has a mixed Co/Ni binder, it has the same melting behavior as alloy # 62. However, the first onset point temperature was not observed for the alloy # 44 due to its much less binder content compared to the alloy # 62.

Cermet alloys # 42 and # 43 are located in the two-phase region of (Ti,W)(C,N)+Co (see Fig.2 (e)). Accordingly, their onset point temperatures measured by DSC are in consistence with the

15th International Plansee Seminar, Eds. G. Kneringer, P. Rödhammer and H. Wildner, Plansee Holding AG, Reutte (2001), Vol. 2

corresponding DTA experimental alloys. However, for TiN cermet alloy # 43 with a hard phase composition of 90 mol% TiN and 10 mol% WC, its onset and peak point temperatures of cooling phase are much different from those of the heating phase (see Fig. 3 and Table 1). Moreover, the strength of the DSC peak during cooling phase is much weaker than that during heating phase. Probably, denitridation was severe for this very high nitrogen-containing alloy so that η was formed during cooling. The formation of η phase consumes the liquid binder phase, which results in different onset and peak point temperatures and weak strength of the peak.

Shrinkage Behaviors

Industrial cermet and cemented carbide alloys are usually sintered in the present of liquid phase. The liquid phase sintering mechanism features three stages: (1) particle re-arrangement, (2) formation of liquid phase and (3) final densification. With respect to the three stages of the liquid phase sintering, three peaks on the DIL $dL/(L_0dt)$%/min curve were observed as shown in Fig.4. The corresponding peak temperatures are listed in Table 2. Samples shrink drastically when particle re-arrangement is observed. In the second sintering stage when liquid phase appears, shrinkage is almost completed as shown by the DIL measurement. In the final stage of the liquid phase sintering, all porosity is removed from the sintered body and full densification is reached. Depending on composition, maximum sintering temperature and sintering parameters, micro-porosity may be residual even after the final stage is completed.

Table 2- Turn point temperatures of some industrial alloys measured by DIL

Alloys	$dL/(L_0dt)$%/min curve; °C			Phase Observed	Remarks
	1st peak	2nd peak	3rd peak		
# 45	1273	1367	-	WC, Co	cemented carbide
# 32	1313	1353	-	WC, (Ti,W)C, Co	cemented carbide
# 35	1303	1359	1407	WC, (Ti,W)(C,N), Co	cemented carbonitride
# 44	1272	1404	1496	WC, (Ti,W)(C,N), Co/Ni	TiCN cermet
# 42	1295	1435	1492	(Ti,W)(C,N), Co/Ni	TiCN cermet
# 43	1301	1436	1510	(Ti,W)(N,C), Co/Ni	TiN cermet

All alloys have nearly the same turn point temperature of about 1300°C for the first peak. For the second peak, alloy # 45, # 32 and # 35 have the same turn point temperature of about 1350°C. The second peak temperature for alloy # 44 is 1400°C. The cermet alloys # 42 and # 43 have the highest turn point temperature of about 1430°C for the second peak. For alloys # 45 and # 32 without nitrogen, the third peak was not obvious. With increased Ti and nitrogen (N) contents, the third peak becomes more significantly in the order of alloy # 35, # 44, # 42 and # 44.

In industrial practice, the sintering temperature should be at least higher than the second peak temperature in order to reach full density. According to the DIL measurements, the optimum sintering temperature will be about 1350-1400°C and 1450-1500°C for industrial cemented carbides (or cemented carbonitrides) and modern cermets, respectively.

15th International Plansee Seminar, Eds. G. Kneringer, P. Rödhammer and H. Wildner, Plansee Holding AG, Reutte (2001), Vol. 2

The liquid phase sintering mechanism is confirmed by comparing DSC measurements with DIL measurements. The particle re-arrangement happens before the formation of liquid phase. The second peak of DIL curves (second stage of the liquid phase sintering) is observed as soon as the liquid phase is detected by DSC (see Table 1, Table 2, Fig.3 and Fig.4).

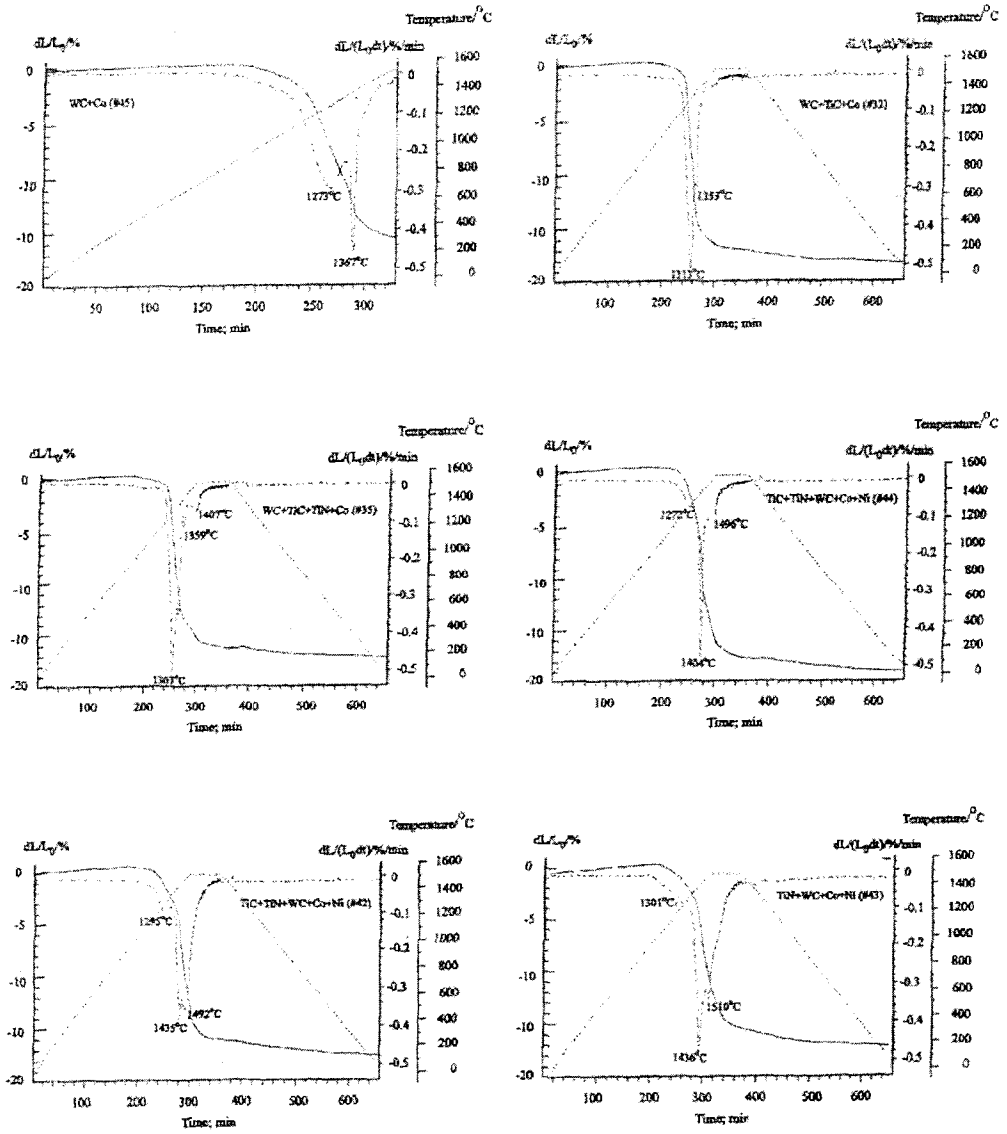

Fig.4- Shrinkage behaviors of some industrial alloys measured by DIL.

15th International Plansee Seminar, Eds. G. Kneringer, P. Rödhammer and H. Wildner, Plansee Holding AG, Reutte (2001), Vol. 2

Gas Evolution during Sintering

As shown in Fig.5 (a), the oxide film on the surface of Co particles is removed below 500°C. Three CO peaks were observed for either pure WC or TiC, because WO_3 and TiO_2 oxides are reduced through three steps: $WO_3 \Rightarrow W_4O_{11} \Rightarrow WO_2 \Rightarrow W$ and $TiO_2 \Rightarrow Ti_2O_3 \Rightarrow TiO \Rightarrow Ti$, respectively. Pure TiN powder is very stable against vacuum up to 1500°C. The gas evolution of WC+TiC powder mixture combines those features of separate WC and TiC powders. However, only two main CO peaks were observed for the WC+TiC powder mixture. Probably, reductions of oxides are easier for the WC + TiC powder mixture than for the separate WC or TiC powders. As for the WC+TiN powder mixture, CO and N_2 peaks were observed at temperatures above 1400°C. Reaction between WC and TiN must happen to release N_2. This is due to the thermodynamic instability of TiN in the present of WC or other carbon source (see the following section).

The gas evolution of some industrial alloys is given in Fig.5 (b). For WC+Co alloy # 45, the outgassing process is almost completed at temperature around 1000°C. Compared to WC+TiC powder mixture, alloy # 32 (WC+TiC+Co) shows lower temperatures of CO outgassing. The effect of Co binder on the mechanism of gas evolution has also been observed for other TiC and/or TiN containing alloys as shown in Fig.5. N_2 peak was not observed for the pure WC+TiN powder mixture below 1400°C. However, in the present of Co and/or Ni binder metals, N_2 starts to release at temperature of about 1200°C for all TiN containing alloys # 35, # 37 and # 42. The gas evolution stops at about 1300°C for all TiC/TiN containing alloys.

During sintering of cermets or cemented carbonitrides, the evolution of CO from chemisorbed or chemically bonded oxygen on the surface of the powder particles, features a few stages at different temperatures around 500°C, 650°C and 1000°C. The different outgassing temperatures correspond to the reductions of different oxides existing on the surface of the powder particles. The main CO peak appears around 1100-1200°C and fades out at about 1250°C. The presence of Co/Ni binder greatly accelerates the elution of CO and therefore improves the removal of the oxide layers from the powder particles. However, denitridation is accelerated by the presence of Co/Ni binder too. The elution of nitrogen sets in at about 1200°C and has a very marked maximum at about 1300°C. With the onset of particle re-arrangement at approximate 1300°C, CO and nitrogen elution drops drastically because of the very strong shrinkage of the compacts. With increasing temperature, the rate of CO and nitrogen elution begin to gradually increase again but only around 1500°C. The formation of liquid phase is not influenced by the starting materials of either pre-alloyed quaternary carbonitrides or powder mixtures of single TiC, TiN and WC. In the range of our experiments, even the stoichiometric factor x of the hard phase $(Ti,W)(C,N)_x$ (x=0.85-1) does not affect the melting point temperatures very much.

Thermodynamic Stability of Hard Phases

The thermodynamic stability of TiC-TiN-WC carbonitrides was studied by X-ray diffractometer (XRD) and the experimental details is given in somewhere else [13-14]. As shown in Fig.6, two f.c.c. (Ti,W)(C,N) phases δ_1 and/or δ_2, where δ_1- $(Ti_x,W_{1-x})(C_{x'},N_{1-x'})$ is rich in Ti, and N and δ_2- $(Ti_y,W_{1-y})(C_{y'},N_{1-y'})$ is rich in W and C, were observed in the whole compositional range of the WC-TiC-TiN hard phase system. Since the composition of the two f.c.c. phases were quite similar, profile fitting with the Difpatan X-ray diffraction program had to be applied to identify the phases. In the

15th International Plansee Seminar, Eds. G. Kneringer, P. Rödhammer and H. Wildner, Plansee Holding AG, Reutte (2001), Vol. 2

composition region A, only one f.c.c. (Ti,W)(C,N) phase was observed. Two f.c.c. phases δ_1 and δ_2 were observed in the compositional region B. In the compositional regions C, D and E, hex-WC, b.c.c.-W and hex-W_2C, respectively, coexisted with δ_1 and δ_2.

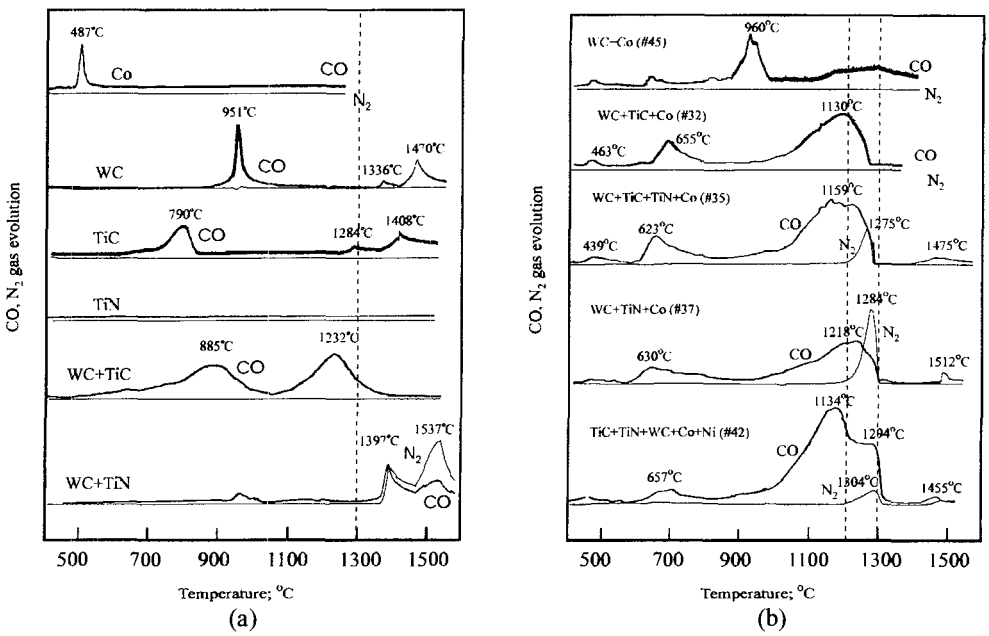

Fig.5- Gas evolution measured by MS during heating of:
(a) pure Co, single carbide/nitride and mixed carbide/carbonitride powders
(b) some industrial alloys.

The TiC-TiN-MoC system can be treated as a reciprocal system: TiC+MoN⇔TiN+MoC according to Rudy [19]. Of particular interest in this system is the phase equilibria within the range of the solid solution $(Ti,Mo)(C,N)_z$ ($0.8 < z < 1$), where, depending upon temperature and composition, a miscibility gap exists featuring two iso-structural phases: α' - a molybdenum poor and nitrogen rich (Ti,Mo)(C,N) phase, and α'' - a molybdenum rich and nitrogen poor (Ti,Mo)(C,N) phase. The separation of these two phases occurs via a spinodal decomposition of a homogeneous solid solution (Ti,Mo)(C,N) that is existent only at high temperatures (Fig.7).

By means of MS analysis given in the previous section, pure TiN was observed to be very stable against vacuum up to 1500°C. However, TiN starts to react with WC (probably Mo_2C too) at about 1350°C, which results in N_2 elution. Moreover, such denitridation reactions are accelerated in the present of Co/Ni binders.

15th International Plansee Seminar, Eds. G. Kneringer, P. Rödhammer and H. Wildner, Plansee Holding AG, Reutte (2001), Vol. 2

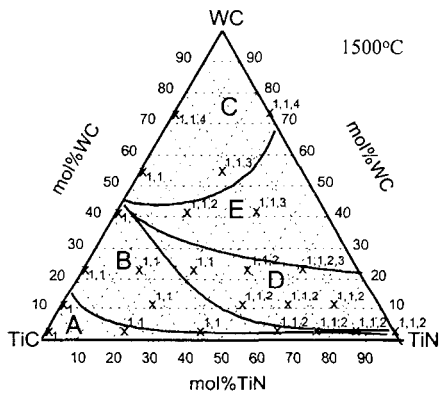

Fig.6- Phase existence in the TiC-TiN-WC hard phase system. All samples were hot-pressed at 2300°C and then Ar-annealed at 1500°C for 168h. The meaning of the numbers in the chart are: 1- f.c.c. phases of δ_1- $(Ti_x,W_{1-x})(C_{x'},N_{1-x'})$ rich in Ti, and N and δ_2- $(Ti_y,W_{1-y})(C_{y'},N_{1-y'})$ rich in W and C; 2- b.c.c W; 3- hex W_2C; and 4- hex WC.

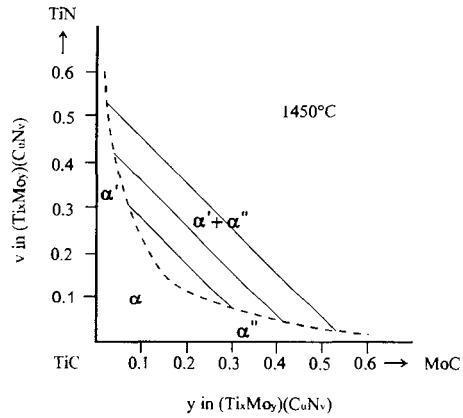

Fig.7- Partial isothermal section of the TiC-TiN-"MoC" hard phase system at 1450°C, after Rudy [19].

It is known that Mo and W do not form nitrides above 1000°C at normal N_2 pressure of 1 bar, and Mo_2C and WC are much more stable against N_2 than TiC and $Ti(C_{1-x},N_x)$. Nitrides tend to decompose under vacuum via evolution of nitrogen. On the other hand, carbides and carbonitrides react with nitrogen under formation of elemental carbon: $<TiC>+1/2N_2 \rightarrow <TiN>+C$. The brackets < > are indicating that TiC and TiN are not separate phases but partners in a solid solution. In that case the three phases equilibrium Ti(C,N), C and gas phase can be formulated in the usual way: $\Delta G=-RT*\ln K_p=-RT*\ln[(a_{TiC}*a_C)/(a_{TiC}*P_{N_2}^{1/2})]$.

Carbon as a phase has the activity $a_C=1$ and if ideality of the solid solution is assumed, then $a_{TiN}/a_{TiC}=x_{TiN}/x_{TiC}$. By introducing the free energies of the formation of TiC and TiN, the equilibrium pressure P_{N_2} in equilibrium with graphite can be calculated for all temperatures and compositions of $Ti(C_x,N_{1-x})$ as illustrated in Fig.8 [20].

Within the two-phase equilibrium: $Ti(C_x,N_{1-x})_z \rightarrow Ti(C_x,N_{1-x})_{z-\Delta z}+1/2z(1-x)\Delta z\ N_2$, the nitrogen partial pressure is a function both of x and z. In the presence of a liquid phase such as Ni or Co, the nitrogen partial pressure will of course influence the solubility of carbon (at carbon activity<1), nitrogen and titanium in the liquid binder metal, and consequently influence the metallurgical reactions. Thus, during the sintering of cermets, nitrogen pressure has to be adjusted within certain limits to the composition of the carbonitrides and the sintering temperature.

15th International Plansee Seminar, Eds. G. Kneringer, P. Rödhammer and H. Wildner, Plansee Holding AG, Reutte (2001), Vol. 2

During sintering of cermets or cemented carbonitrides, as soon as the oxide film on the powder particles has been removed by the reductive processes, wetting by the binder metal melt sets in and the carbon-containing binder metal melt interacts with the hard phase particles. As could be demonstrated in investigations by Kieffer et. al. [1], depending on the nitrogen pressure in the sintering atmosphere, carbon is able to displace nitrogen from the nitrides (at low nitrogen partial pressure) or nitrogen is able to displace carbon from the carbides. The nitrogen equilibrium pressure of titanium carbonitride in equilibrium with elementary carbon is, apart from the temperature, only determined by the composition of the carbonitride. If the carbon activity becomes <1, i.e. if the carbon supplier is a carbide e.g. Mo_2C or WC, the corresponding nitrogen equilibrium pressure is slightly reduced. Fig.8 shows which nitrogen pressures are to be expected at least in the initial phases of the sintering process, i.e. when the carbon-containing liquid phase begins to react with the surface of the nitride or carbonitride particles. If the nitrogen partial pressure is considerably below the limits for quite a long time during sintering, it can be assumed that considerable amounts of titanium will be dissolved in the binder alloy so that the precipitation of intermetallic phases of the type Ni_3Ti might finally be the consequence [20].

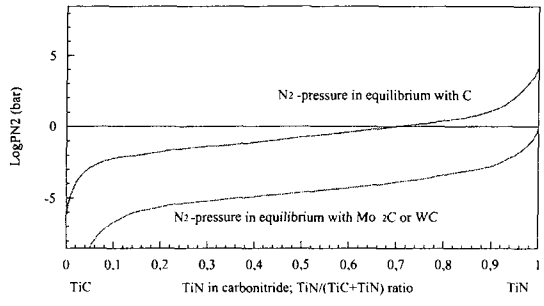

Fig.8- Nitrogen equilibrium pressure of titanium carbonitride of different compositions at 1450°C, after Ettmayer et.al. [20].

The carbides of the IVth group metals and VC_{1-x} react readily with nitrogen under formation of a carbonitride and graphite. The compositions of the carbonitrides are dependent on nitrogen pressure and temperature of reaction. As predicted by thermodynamics, higher pressure of nitrogen leads to carbonitrides richer in nitrogen, at higher temperatures otherwise under identical conditions the nitrogen content in the carbonitrides becomes lower. NbC and Mo_2C react only to a very small extent with nitrogen, whereas TaC and WC appear to be stable against nitrogen even at very high pressures. Cr_3C_2 reacts with nitrogen of 300 bar under formation of a ternary compound $Cr_3(C,N)_2$ as reported by Kieffer and Ettmayer et. al. [21].

Phase Reactions

Through XRD measurements, Yoshimura et.al studied phase reactions of a cermet with a composition of TiC-20%TiN-15%WC-10%TaC-9%Mo-5.5%Ni-11%Co [22]. The relative XRD intensities (I/I_0) and lattice parameters of each phase as functions of sintering temperature are re-given in Fig.9. The intensity (I/I_0) of TiC increases with increasing temperature, most remarkably in the range of 1100-1200°C. In the meantime, the intensities (I/I_0) of Mo_2C, TaC, WC, and TiN decrease. Correspondingly, the lattice parameter of TiC phase decreases, and the lattice parameter of the binder phase increases respectively. This fact means that Mo_2C, TaC, WC, and TiN phases have

15th International Plansee Seminar, Eds. G. Kneringer, P. Rödhammer and H. Wildner, Plansee Holding AG, Reutte (2001), Vol. 2

considerably dissolved in TiC and binder phase. The Mo_2C phase dissolves most rapidly and completely disappears already at 1200°C. TaC and WC phases disappear at 1300°C. TiN dissolves more slowly in comparison with Mo_2C, TaC, and WC. A certain amount of TiN still remains undissolved even at temperatures as high as 1400°C. The dissolution of Mo_2C, TaC, WC, and TiN observed at temperatures below 1300°C must have taken place through solid state diffusion, since liquid phase starts to appear first at approximately 1300°C.

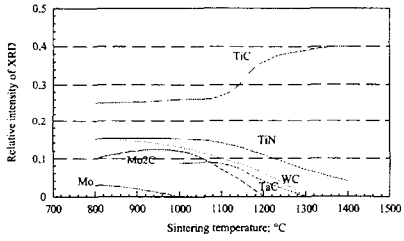

Fig.9 (a)- Relative intensities of XRD of Mo, Mo_2C, TaC, TiN and TiC vs. sintering temperature [22].

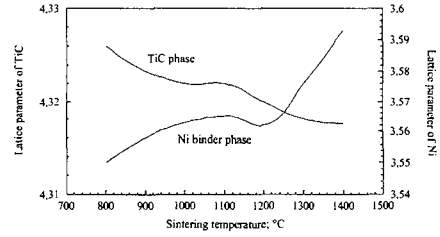

Fig.9 (b)- Lattice parameters of TiC and Ni binder phase vs. sintering temperature [22].

The solubility of the metal components of the carbides (and nitrides) in the binder metals is very much influenced by the stoichiometry of the carbides (or nitrides). Whenever the carbon activity is low (sub-stoichiometry), the solubility of the metal component can be rather high. Some solubility data are listed in Table 3 [23-24].

Table 3- Solubility of hard phases in liquid and solid metals [23-24]

Solubility of hard phases in liquid metals at 1400°C after Ettmayer et. al. [23]			Solubility of hard phase in solid binder metals at 1250°C after Edwards et. al. [24]		
Hard phase	in Ni; wt%	in Co; wt%	in Ni; wt%	in Co; wt%	in Fe; wt%
TiC	11	10	1	5	<0.5
TiN	< 0.5	< 0.5	<0.1	<0.1	<0.1
Mo_2C	36	39	13	8	5
WC	27	39	22	12	7
TaC	6.3	6.3	3	5	0.5
NbC	7.0	8.5	5	3	1
VC	14	19	-	-	-
Cr_3C_2	-	-	12	12	8

15th International Plansee Seminar, Eds. G. Kneringer, P. Rödhammer and H. Wildner, Plansee Holding AG, Reutte (2001), Vol. 2

On the cross sections of "solid-liquid" reaction couples, four different zones were observed: (1) un-reacted carbide compact; (2) diffusion zone where the liquid metal has penetrated along the grain boundaries; (3) reaction zone and (4) metal alloy zone where the metal melt has solidified and the carbide has re-precipitated from the melt. An example of such cross section is given in Fig.10. On one hand, Ti, Mo/W and C atoms dissolve from carbide compact into the Ni/Co melt. On the other hand, the Ni/Co metal melt penetrates into the carbide compact along the grain boundaries, which gives rise to penetration of liquid deep into the carbide compact and the formation of a reaction zone where melt and undissolved carbide particles coexist. Upon cooling down, dissolved Ti, Mo/W and C atoms re-precipitate in the form of mixed carbide in the Ni/Co melt region, and eventually the Ni/Co melt solidifies, too. In the reaction zone, part of the compact carbides goes into solution of the Ni/Co melt and - on cooling - re-precipitates as mixed carbide, whereas part of the original carbide remains un-dissolved. The undissolved carbides in the reaction zones contain less Mo than the original carbides.

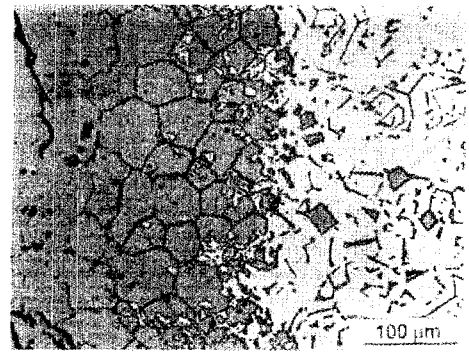

Fig.10- Microstructure of the cross section of $(Ti_{0.9},Mo_{0.1})C$-Ni solid-liquid reaction couple; 200x

"Selective dissolution and selective re-precipitation" of heavy elements during "solid-liquid" reactions were observed by SEM/EDS as shown in Fig.11. They are probable the result of the fact that different carbides have quite different solubility in the Co/Ni binder metals (see Table 3). Because of the selective dissolution of Mo (or W) from the solid carbide compact, the melt contains relatively more Mo (W) than the carbide compact in equilibrium with it. Hence, upon solidification (cooling down), the precipitating carbide and/or Ni/Co phase must contain relatively more Mo (W) than the starting carbide compact in contact with the melt.

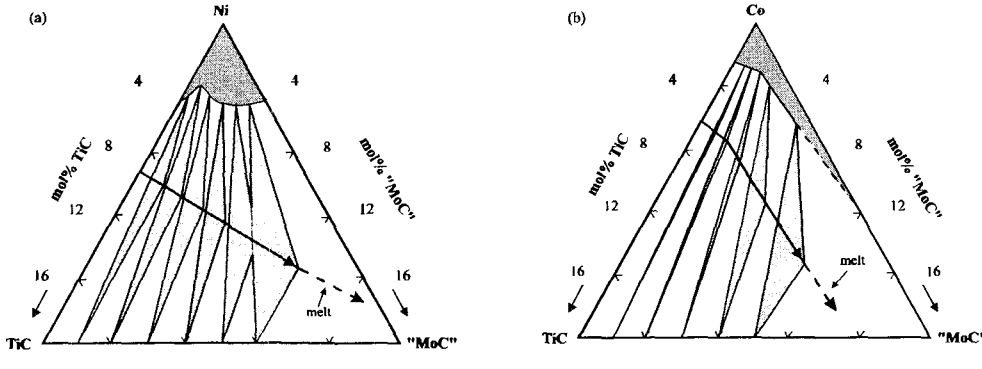

Fig.11- Phase equilibria between melt, (Ti,Mo)C carbide and Ni/Co solid solution in solid/liquid reaction couples of (a) Ni-(Ti,Mo)C near 1300°C and (b) Co-(Ti,Mo)C near 1350°C.

15th International Plansee Seminar, Eds. G. Kneringer, P. Rödhammer and H. Wildner, Plansee Holding AG, Reutte (2001), Vol. 2

The interactions between hot-pressed (Ti,W)(C,N) compacts and N_2 up to 30 bars have been studied for the entire compositional range of the TiC-TiN-WC system [13]. An example of the results is given in Fig.12. Upon N_2 pressure, temperature and chemical composition, the quaternary (Ti,W)(C,N) alloys may decompose into two f.c.c. phases δ_1 and δ_2 and WC through: (Ti,W)(C,N) + $N_2 \rightarrow \delta_1 + \delta_2 +$ WC, where δ_1-$(Ti_x,W_{1-x})(C_{x'},N_{1-x'})$ is rich in Ti, and N and δ_2-$(Ti_y,W_{1-y})(C_{y'},N_{1-y'})$ is rich in W and C (see Fig.6). In the microstructure of un-attached area, δ_1-$(Ti_x,W_{1-x})(C_{x'},N_{1-x'})$ is darker than δ_2- $(Ti_y,W_{1-y})(C_{y'},N_{1-y'})$ as shown in Fig.12 (a). The original (Ti,W)(C,N) grains near the surface were attacked by N_2 to form very fine structures where WC phase (white and very thin in shape) was observed. The element distributions across sample section show gradients of C, N and W (see Fig.12 (b)). N concentration decreases while C and W concentrations rise with increasing distance from the sample surface.

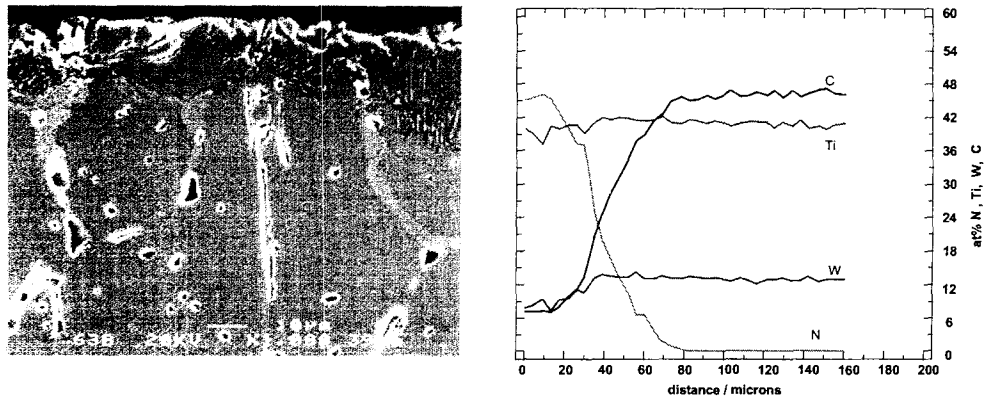

(a) SEM back scatter images (b) EPMA measurement

Fig.12- (a) SEM microstructure and (b) element distribution of the surface interaction zone of a hot-pressed (Ti,W)(C,N) sample after N_2 annealing at 1500°C and 30 bar N_2 (WC/TiC/TiN = 24/76/0 in mol%;)

Mechanism of Formation of "Core-Rim" Structures in Cermets

"Core-rim" structure within the hard phases is the typical microstructure of cermets. As shown in Fig.13, hard particles with "bright core-dark rim", or with "bright rim-dark core" can be observed. Some hard particles even have complex structure with an inner rim. Element analysis across the Ni binder phase and carbide grains was carried out by TEM/EDS. The compositions and preparation processes of TEM specimens are listed in Table 4. Fig.14 gives a photograph of sample 6N. The white particles are hard phase and the gray areas are Ni binder phase. The dark spots in the microstructure are the points where chemical compositions were analyzed by TEM/EDS. Mo-rich rims are clearly demonstrated in Fig.15.

Ti, Mo concentrations in the Ni binder phase are probably controlled by the stoichiometry factor z as well as by the nitrogen content of the hard phases. Decreasing of the stoichiometry factor z will improve the solubility of Ti and Mo, while increasing of nitrogen content in the hard particles will

15th International Plansee Seminar, Eds. G. Kneringer, P. Rödhammer and H. Wildner, Plansee Holding AG, Reutte (2001), Vol. 2

decrease the Ti concentration but largely increase the Mo concentration. Sample TM8102 has a stoichiometric carbide $(Ti_{0.8},Mo_{0.2})C$, P4 has a sub-stoichiometric carbide $(Ti_{0.8},Mo_{0.2})C_{0.9}$, while 6N has a slightly sub-stoichiometric carbonitrides phase $(Ti_{0.8},Mo_{0.2})(C_{0.7},N_{0.3})_{0.97}$. As shown in Fig.16, the Ti, Mo concentrations and the total amount (Ti+Mo) in the Ni solid solution of sample P4 are nearly double that of TM8102. Sample 6N has a much higher Mo content and a lower Ti content than those of both P4 and TM8102. The total amount of (Ti+Mo) in the binder phase of 6N is similar to that of P4, but higher than that of TM8102.

Table 4- Compositions and preparing process of TEM specimens

Samples	Chemical compositions	Starting materials	Preparing process
TM8102	$(Ti_{0.8},Mo_{0.2})C$ + 50 vol% Ni	$(Ti_{0.8},Mo_{0.2})C$; Ni	Vacuum sintered; 1h. 1400°C, 8×10^{-2} mbar
P4	$(Ti_{0.8},Mo_{0.2})C_{0.9}$ + 18 mol% Ni	TiC, Mo_2C, C, Ni	Vacuum sintered; 1h. 1500°C, 10~20 mbar
6N	$(Ti_{0.8},Mo_{0.2})(C_{0.7},N_{0.3})_{0.97}$ + 18 mol% Ni	$(Ti_{0.8},Mo_{0.2})(C_{0.7},N_{0.3})_{0.97}$, Ni	Vacuum sintered; 1h. 1500°C, 80 mbar N_2

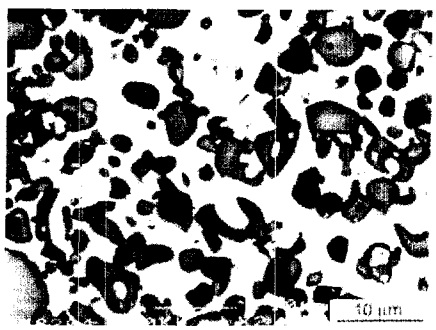

Fig.13- "Core-rim" structure in sample TM8102 observed by SEM back scatter image.

Fig.14- TEM image of sample 6N with EDS analysis spots (dark); 20,000x

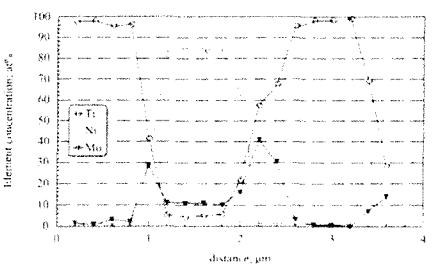

Fig.15- Element distribution across grains of 6N specimen.

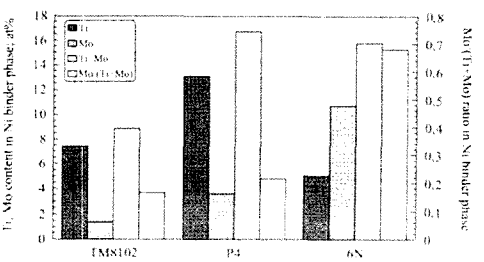

Fig.16- Binder phase compositions of TM8102, P4 and 6N

15th International Plansee Seminar, Eds. G. Kneringer, P. Rödhammer and H. Wildner, Plansee Holding AG, Reutte (2001), Vol. 2

During sintering we can assume that quasi-isothermal conditions will prevail and in the ideal case of equilibration we will end up with a binder melt somewhat higher in Mo (or W if WC is present, the same for the follows) than the carbides in equilibrium with the melt. In reality we will have non-equilibrium conditions because the diffusivities in the carbide phase are lower by several orders of magnitude than the diffusivities in the liquid phase. Furthermore, the rates of dissolution will depend on the grain sizes of the carbide particles. During liquid phase sintering of a cermet alloy, it can be anticipated that in the first few minutes of liquid phase formation the small particles of (Ti,Mo)C will go into solution at a higher rate than the larger particles. Since this constitutes a non-equilibrium condition (the melt has the same Ti/(Ti+Mo) atom ratio as the carbide phase), a Mo depleted (Ti,Mo)C will start to re-precipitate, probably epitaxially, on some favourable lattice sites of un-dissolved larger (Ti,Mo)C particles. Because of this re-precipitation, some more (Ti,Mo)C particles will go into solution and some more Mo-depleted (Ti,Mo)C particles will precipitate. If that Mo-depleted (Ti,Mo)C phase on re-precipitation completely surrounds a large original (Ti,Mo)C particle and seals it off from the action of the liquid phase we will end up with a "bright core - dark rim" microstructure. If, on the other hand, the re-precipitated Mo-depleted (Ti,Mo)C nucleates only on one favourable nucleation site of an original (Ti,Mo)C particle, the original particle will gradually be eaten away by the liquid and only during the cooling down period the Mo-rich liquid will form a Mo-rich (Ti,Mo)C rim (bright) around the Mo-depleted core ("dark core - bright rim" microstructure). By such mechanism the simultaneous occurrence of the two types of hard particles with bright cores and dark rims or with bright rims and dark cores might be explained. Furthermore, it is highly doubtful whether any supplier of pre-alloyed carbide material will really be able to provide a completely homogeneous pre-material without **any** compositional gradients. Inhomogeneous pre-materials obviously will lead to somewhat inhomogeneous microstructural features.

Phase Observation and Grain Size

The microstructure of cermets or cemented carbonitrides is determinated by the compositions of their hard phases in the WC-TiC-TiN and/or WC-TiCN-TaC systems (see Fig.2 (e) and (f)). If the hard phase composition of an alloy is located in the cermet compositional range of (Ti,W)(C,N)+Co/Ni, WC phase will not be observed. On the other side, WC phase will be observed in the cemented carbonitride range of WC+(Ti,W)(C,N)+Co/Ni. In fact, the existence of WC phase in the microstructure is the result that WC has a maximum solubility in the cubic phases of TiC and TaC. The solubility of WC in TiC and TaC is about 40 mol% and 10 mol%, respectively (see Fig.2 (e)-(f) and Fig.6). Fig.17 gives a micrograph of a sample with hard phase composition in the WC+(Ti,W)(C,N)+Co/Ni range of WC/TiC=42/58 (in mol%). The microstructure is composed of faceted WC with large elongated grains and a spherical "core-rim type" (Ti,W)C with a Ti-rich core. Because almost all WC has dissolved into TiC, only a few un-dissolved WC grains were observed in the microstructure.

As to nitrogen-containing cemented carbonitrides and cermets, TiN usually acts as a grain growth inhibitor and produces very fine-grained microstructures with a spherical tungsten-rich phase. Generally, the grain size of the hard phases decreases with increasing N/(C+N) content of the alloy. Upon increase of the TiN content, the WC-rich (or pure WC) phase becomes much less faceted and the surface of the particles gets irregular with shape of these particles being spherical. The (Ti,W)(C,N) phase also has a "core-rim" type structure though the individual grains can hardly be

15th International Plansee Seminar, Eds. G. Kneringer, P. Rödhammer and H. Wildner, Plansee Holding AG, Reutte (2001), Vol. 2

seen at low magnification. Moreover, the WC phase content in the microstructure increases if the N/(C+N) ratio of the alloys increases. An example of a N-containing alloys is given in Fig.18.

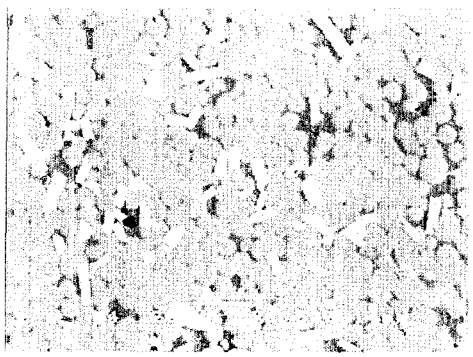

Fig.17- SEM image of an alloy sample (WC/TiC=42/58 in mol%; without nitrogen). Coarse-grained microstructure with faceted bright WC grains.

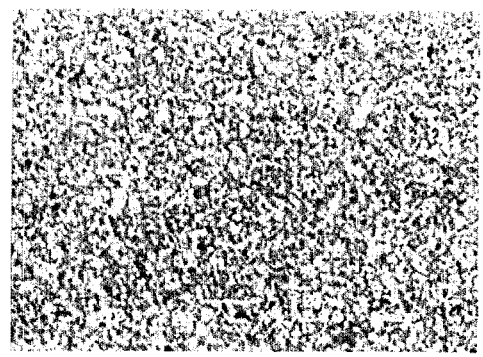

Fig.18- SEM image of an alloy sample (WC/TiC/TiN = 55/25/20 in mol%). Fine-grained structure of both the WC-rich and TiC-rich phase.

Surface Modification through Sintering

Different types of Functionally graded cemented carbonitrides (FGCC) have been prepared through direct sintering by careful alloy design and process (especially atmosphere) control. Some examples of the FGCC microstructures are given in Fig.19-21.

Fig.19 (a) shows a typical CFL layer covering the entire surface of the insert. By modifying the sintering atmosphere, CFL substrate with more cubic phase enrichment in the cutting edge can be prepared (see Fig.19 (b)). The composition of the starting materials can be either nitrogen-containing (Ti,W)(C,N)+Co/Ni green compacts, or non nitrogen-containing (Ti,W)C+Co/Ni green compacts with nitrogen pre-treating.

Another type of FGCC material features a cubic phase rich, WC phase free cermet surface layer which has compositional gradients of Ti, W, Co, C and N up to 500 μm, depending on the overall composition of the alloy. Fig.20 (a) gives an example of the microstructure of such FGCC material with high wear-resistant cermet surface, high tough cemented carbonitride substrate. Gradation of chemical composition was observed in the surface layer as shown in Fig.20 (b) measured by GDS. The experimental details of GDS measurement are given in [12-13]. The depth of the compositional gradient of this alloy is about 30 μm.

Even multi-layered FGCC insert materials can be fabricated by direct sintering. As shown in Fig.21, the as-sintered material consists of a TiCN high wear-resistant outermost surface, a CFL underneath WC+Co tough intermediate layer and cemented carbonitride strong core. Materials with similar surface modification must be prepared by costly CVD or PVD [6] before direct sintering technology

15th International Plansee Seminar, Eds. G. Kneringer, P. Rödhammer and H. Wildner, Plansee Holding AG, Reutte (2001), Vol. 2

developed in this work. Because of the graded structures within each layer as shown in Fig.21 (b), this new type insert material is believed even to outperform "state-of-the-art" coated cemented carbides.

(a) (b)

Fig.19- Microstructures of cross sections of some cemented carbonitrides. (a) entire CFL surface layer; (b) CFL surface layer with cubic phase enriched cutting edge.

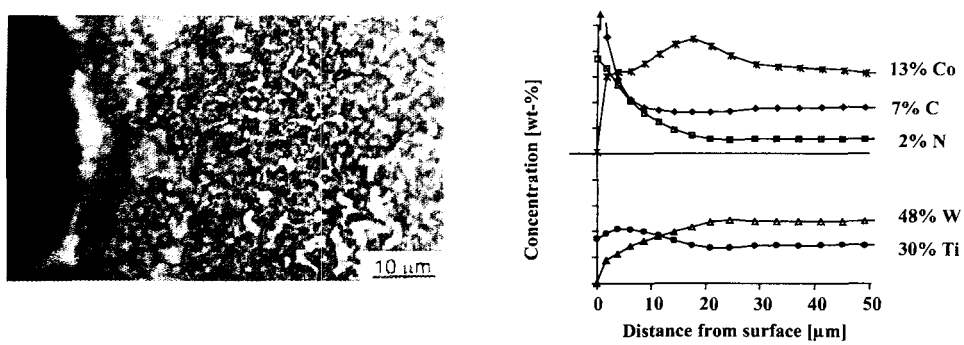

(a) (b)

Fig.20- FGM cermet surface layer on a cemented carbonitride substrate: (a) microstructure of the cross section and (b) GDS depth analysis (experimental details of GDS is given in [12-13]).

15th International Plansee Seminar, Eds. G. Kneringer, P. Rödhammer and H. Wildner, Plansee Holding AG, Reutte (2001), Vol. 2

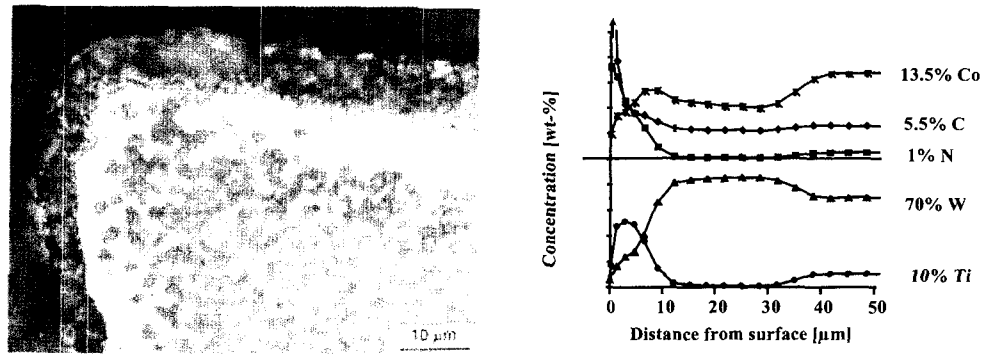

(a) (b)

Fig.21- Microstructure of a cemented carbonitride with multi-layered FGM surface: (a) microstructure of the cross section and (b) GDS depth analysis.

CONCLUSIONS

- Melting behaviors of cermet and cemented carbonitride alloys have been studied by DTA and DSC. Regardless of their Ti/W ratios and C/N ratios, the WC+(Ti,W)(C,N)+Co cemented carbonitrides have a constant melting point temperature of 1350°C. (Ti,W)(C,N)+Co cermets have melting point temperatures in the range of 1350-1450°C, depending on C/N ratios of the alloy.
- During liquid phase sintering, particle re-arrangement of all (Ti,W)(C,N)+Co cermets and WC+(Ti,W)(C,N)+Co cemented carbonitrides start to begin at about 1300°C. Liquid phase sintering was observed by DIL at 1350°C and 1400-1450°C for industrial cemented carbonitrides and cermets, respectively.
- Gas evolution was investigated by MS. Oxide films on the surface of particles are almost reduced below 1300°C. Outgassing process stops at 1300°C as soon as particle re-arrangement starts.
- TiN is very stable against vacuum up to at least 1500°C. In the present of carbon source such as WC, Mo_2C and graphite, denitridation was observed. The denitridation is acerbated through Co/Ni binder metals because of enhanced diffusion through binder metals.
- Thermodynamic stability of hard phases, phase reactions and phase equilibria within WC-TiC-TiN system have been studied.
- Insert materials with different surface modifications have been prepared by direct sintering. As-sintered inserts are believed to compete or even outperform traditional coated carbides.

15th International Plansee Seminar, Eds. G. Kneringer, P. Rödhammer and H. Wildner, Plansee Holding AG, Reutte (2001), Vol. 2

ACKNOWLEDGMENTS

The authors would like to acknowledge Widia GmbH, Germany and Austrian Academic Exchange Service (OEAD) for partially financial support of the research. Very valuable discussions and information exchange from Dr. van den Berg, Dr. Dreyer, Dipl-Ing. Kassel and Dipl.-Ing. Daub of Widia GmbH are greatly appreciated. Thanks are also due to Dr. Sejc, Dipl-Ing. Garcia, Mr. Kral of TU-Wien and Ing. Trampert of ARCS Seibersdorf, Austria, for their contribution to some of the experiments. Dr. Limin Chen would also like to thank his wife Dr. Hua Ge and Mr. Cippel of SinterMet, LLC. for their assistance during the preparation of the manuscript.

REFERENCES

1. R. Kieffer, P. Ettmayer and M. Freudhofmeier: "About Nitrides and Carbonitrides and Nitride-Based Cemented Hard Alloys", Modern Development in Powder Metallurgy, Vol. 5, p. 201-214, edited by H. Hausner, 1971.
2. P. Ettmayer and W. Lengauer: "The Story of Cermets", Powder Metallurgy International, Vol.21, No.2, p. 37-38, 1989.
3. H. Pastor: "Titanium Carbonitride Based Hard Alloys for Cutting Tools", Materials Science and Engineering, A105/106, p. 401-409, 1988
4. P. Ettmayer, H. Kolaska, W. Lengauer and K. Dreyer: "Ti(C,N) Cermets – Metallurgy and Properties", Int. J. Refract. Met. & Hard Meter. Vol.13, p. 343, 1995
5. H. Doi: "Advanced TiC and TiC-TiN based cermets" Proc. Of the 2nd Int. Conf. Science of Hard Materials, p. 489-523, 1986.
6. H. van den Berg, U. Konig, V. Sottke, R. Tabersky and H. Westphal: "Die Bedeutung von modifizierten Randzonen fur die Hartmetallbeschichtung", in "Hartstoffe, Hartstoffschichten, Werkzeuge, Verschleissschutz" of Pulvermetallurgie in Wissenschaft und Praxis Band 13, p. 77-87, edited by R. Ruthardt, Published by Werkstoff-Informationsgesellschaft mbH, 1997.
7. H. Suzuki, K. Hayashi and Y. Taniguchi: "The β-Free Layer near the Surface of Vacuum-Sintered WC-β-Co Alloys Containing Nitrogen", Transactions of the Japan Institute of Metals, Vol 22, No.11, p. 758-764, 1981.
8. W. C. Yohe: "The development of Cubic-Carbide-Free Surface Layers in Cemented Carbides without Nitrogen", Proceedings of the 13th International Plansee seminar, Eds. H. Bildstein and R. Eck, metallwerk plansee, Vol.2, p. 151-168, 1993.
9. M. Schwarzkopf, H. E. Exner and H. F. Fischmeister: "Kinetics of Compositional Modification of (W,Ti)C-WC-Co Alloy surfaces", Materials Science and Engineering, A105/106, p. 225-231, 1988.
10. K. Hayashi, H. Suzuki and Y. Doi: "Effect of β-free Layer of Substrate on properties of Cemented Carbide Coated with TiC by CVD Process", Journal of Japan Society of Powder and Powder Metallurgy, Vol. 32, No. 7, p. 28-31, September, 1985.
11. K. Tsuda, A. Ikegaya, K. Isobe, N. Kitagawa and T. Nomura: "Development of Functionally Graded Sintered Hard Materials", Powder Metallurgy, Vol. 39, No.4, p. 296-300, 1996.

15th International Plansee Seminar, Eds. G. Kneringer, P. Rödhammer and H. Wildner, Plansee Holding AG, Reutte (2001), Vol. 2

12. L. Chen and W. Lengauer: "Metallurgical Mechanisms and Processing Technologies of FGM (Ti,W)(C,N)-Co Hardmetals", Internal reports of Austrian Research Center, OEFZS-A—4185, September. 1997
13. L. Chen and W. Lengauer: "Metallurgical Mechanisms and Processing Technologies of FGM (Ti,W)(C,N)-Co Hardmetals", Internal reports of Austrian Research Center, OEFZS-A—4516, Nov. 1998
14. L. Chen, W. Lengauer and K. Dreyer: "Advances in Modern Nitrogen-Containing Hardmetals and Cermets", Proceeding of the European Conference on Advances in Hard Materials Production sponsored by EHMG & EPMA, Turin, Italy, p. 463-473. November 8-10, 1999.
15. W. Lengauer, L. Chen, J. Garcia, V. Ucakar, K. Dreyer, D. Kassel and H. W. Daub: "Diffusion-Controlled Surface Modification of Functionally-Gradient (Ti,W)C-Based Cemented Carbonitrides", Proceedings of the 1999 International Conference on Powder Metallurgy & Particulate Materials sponsored by the Metal Powder Industries Federation and APMI international, Vol. 3, Part 10, p.85-96, June 20-24, 1999, Vancouver, B.C. Canada,
16. L. Chen, W. Lengauer, H. W. Daub, K. Dreyer and D. Kassel, German Patent DE 198 45 376 A1, January 13, 2000.
17. K. Dreyer, W. Daub, H. Holzhuer, S. Orths, D. Kassel and K. Rodiger: "Trends in der Hartmetallfertigung: Legierungen, Verfahren, Produkte", in "Hartstoffe, Hartstoffschichten, Werkzeuge, Verschleissschutz" of Pulvermetallurgie in Wissenschaft und Praxis Band 13, p. 3-27, edited by R. Ruthardt, Published by Werkstoff-Informationsgesellschaft mbH, 1997.
18. P. Ettmayer, H. Kolaska and K. Dreyer: "Effect of the Sintering Atmosphere on the Properties of Cermets", Powder Metallurgy International, Vol.23, No.4, p. 224-229, 1991.
19. E. Rudy: "Boundary Phase Stability and Critical Phenomena in Higher Order Solid Solution Systems", Journal of the Less-Common Metals. Vol. 3, p. 343-70, 1973.
20. P. Ettmayer, H. Kolaska and K. Dreyer: " Effect of the Sintering Atmosphere on the Properties of Cermets", pmi Vol. 23, No. 4, p. 224-230, 1991.
21. R. Kieffer and P. Ettmayer: "Grundlagen und Neuentwicklungen auf dem Gebiet metallischer und nichtmetallischer Hartstoffe", Chemie-Ing.-Tech. 42 Jahrg. /Nr. 9/10, p. 589-599, 1970.
22. H. Yoshimura, T. Sugizawa, K. Nishigaki and H. Doi: "Reaction Occurring During Sintering and the Characteristics of TiC-20TiN-15WC-10TaC-9Mo-5.5Ni-11Co Cermets", R&HM December 1983, p. 170-174.
23. P. Ettmayer, H. Kolaska, W. Lengauer und K. Dreyer: " Cermetlegierungen-Metallurgie und Eigenschaften", Proceedings of the 13th. International Plansee Seminar '93, HM2, Vol. 4, p. 191-208, May 24-28, 1993, Tirol, Austria.
24. R. Edwards and T. Raine: "The Solid Solubility of Some Stable Carbides in Cobalt, Nickel and Iron at 1250°C", Proc. 1st Int. Plansee Seminar, p. 232, 1952.